



Bunch-by-bunch studies at DELTA

NOVEMBER 17–19, 2009

Author:
Dmitry TEYTELMAN

Revision:
1.2

March 30, 2010

Copyright © Dimtel, Inc., 2010. All rights reserved.

Dimtel, Inc.
2059 Camden Avenue, Suite 136
San Jose, CA 95124
Phone: +1 650 862 8147
Fax: +1 603 907 0210
www.dimtel.com

Contents

1	Introduction	2
1.1	Feedback Hardware Configuration	2
2	Results	4
2.1	Back-end timing	4
2.2	Measurements under the instability threshold	5
2.3	Measurements above the threshold	8
2.4	Transverse measurements	10
3	Simulation	12
3.1	Model	12
3.2	Simulated grow/damp	13
3.3	Steady-state noise	15
3.4	Extrapolation	17
4	Summary	17
5	Glossary	20

Table 1: DELTA parameters

Parameter description	Symbol	Value
Nominal RF frequency	f_{RF}	500 MHz
Harmonic number	h	192
Momentum compaction	α	5.3×10^{-3}
Beam energy	E_0	1.482 GeV
Radiation damping time, longitudinal	τ_{rad}	4.17 ms

1 Introduction

During the week of November 16–20, 2009, bunch-by-bunch feedback system from Dimtel, Inc. [1] was demonstrated at DELTA storage ring. This brief note summarizes the results of the coupled-bunch instability studies performed in the course of this demonstration.

DELTA is a 3rd generation light source operated by Technical University of Dortmund, Germany. Main parameters of DELTA during our studies are listed in Table 1.

1.1 Feedback Hardware Configuration

The most challenging aspect of the demonstration at DELTA was finding a way to apply feedback correction signal to the beam. The only device even remotely suitable to the task was a single diagonal stripline normally used for tune measurements [2]. The stripline is driven on the upstream end and is grounded on the downstream side. Stripline length l is roughly 0.4 m. The longitudinal shunt impedance of such structure has frequency dependence of the form $\sin(\omega l/c)^2$ with periodic peaks at $nc/4l$. Expected peak shunt impedance is quite low, given that the beam is only kicked by a single stripline with the signal reflected from the downstream end of the line. In addition, from the sketch of the kicker structure shown in Fig. 1 and the description presented in [3] it seems likely that the line impedance is much lower than 50Ω .

Generating excitation for such a kicker is difficult for several reasons. Grounded stripline reflects all of the amplifier output power back to the source. The reflection is combined with the beam-induced power. A way to protect the amplifier from the reverse power is a must. Additionally,

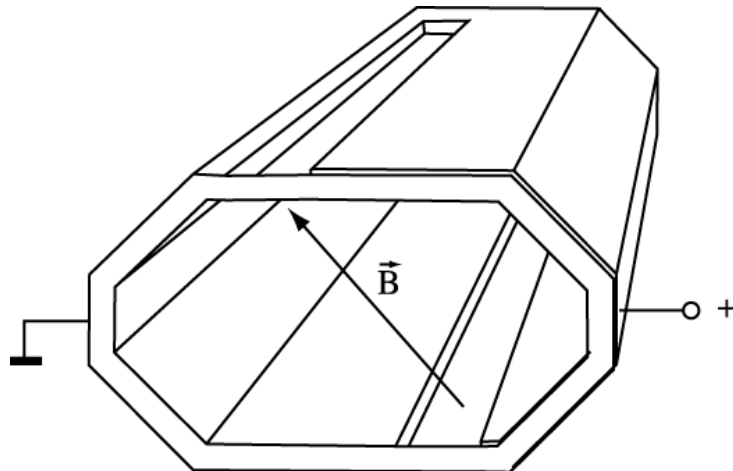


Figure 1: Sketch of the diagnostic stripline in DELTA.

since only a single stripline is driven, kicking at baseband would excite the beam both longitudinally and transversely, albeit at low amplitudes in the transverse planes due to tune separation.

To achieve all of the above goals, it was decided to use the shunt impedance peak at $5c/4l$ or 937.5 MHz. Resulting back-end setup is shown in Figure 2. Milmega 220 W 0.8–2.2 GHz power amplifier was used as the power source. Four amplifier outputs were combined and passed through a circulator and a directional coupler before driving the stripline. Reflected and beam induced power was directed by a circulator to a 500 W load, thus protecting the power amplifier output. A calibrated directional coupler was used to monitor reflected signals.

The power amplifier was driven by the FBE-500L longitudinal back-end [4]. The back-end unit modulates the amplitude of the $2 \times f_{\text{RF}}$ carrier with the baseband feedback kick signal. Such modulation places most of the power between 750 MHz and 1.25 GHz. In a standard configuration a bandpass filter centered at 1.125 GHz emphasizes the upper sideband. For the test at DELTA the bandpass filter was configured for wide bandwidth, allowing us to drive the kicker with the lower sideband of 1 GHz.

Beam-induced signals, coupled out by Narda 3001-20 directional coupler were monitored using a spectrum analyzer and a wideband oscilloscope. With a short bunch train in the ring the spectrum analyzer showed a peak centered at 955 MHz, suggesting that the actual stripline length is 39.3 cm — very

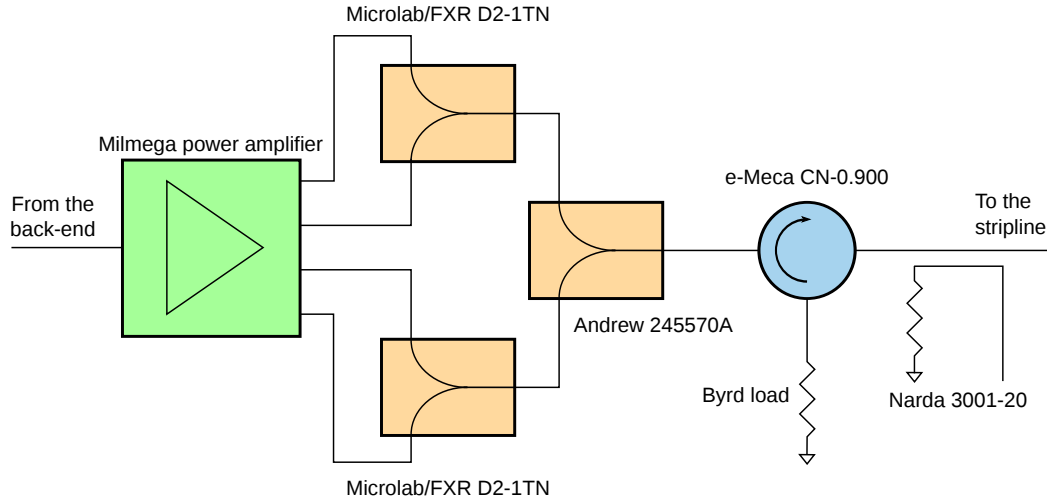


Figure 2: Back-end high-level setup.

close to our original estimate of 40 cm.

2 Results

The main focus of our measurements was on quantifying the longitudinal coupled-bunch instabilities in DELTA. However some parasitic measurements of the transverse instabilities were performed as well. In this section measurement process and results are summarized.

2.1 Back-end timing

In the back-end timing procedure we excite the beam at the synchrotron resonance with a sinewave and measure the response as a function of kick timing. For this procedure it is desirable to fill as short a bunch pattern as possible. In DELTA we used a train of roughly 8 bunches with very low total current — in fact the current monitor read 0.0 mA. Magnitude of the spectral peak at the synchrotron frequency is plotted versus back-end delay in Figure 3. Flat-top of four RF buckets is related to the length of the filled bunch train. Based on the sweep the optimal timing is midway between 121 and 122 settings. To achieve that value we set the delay adjustment to 121

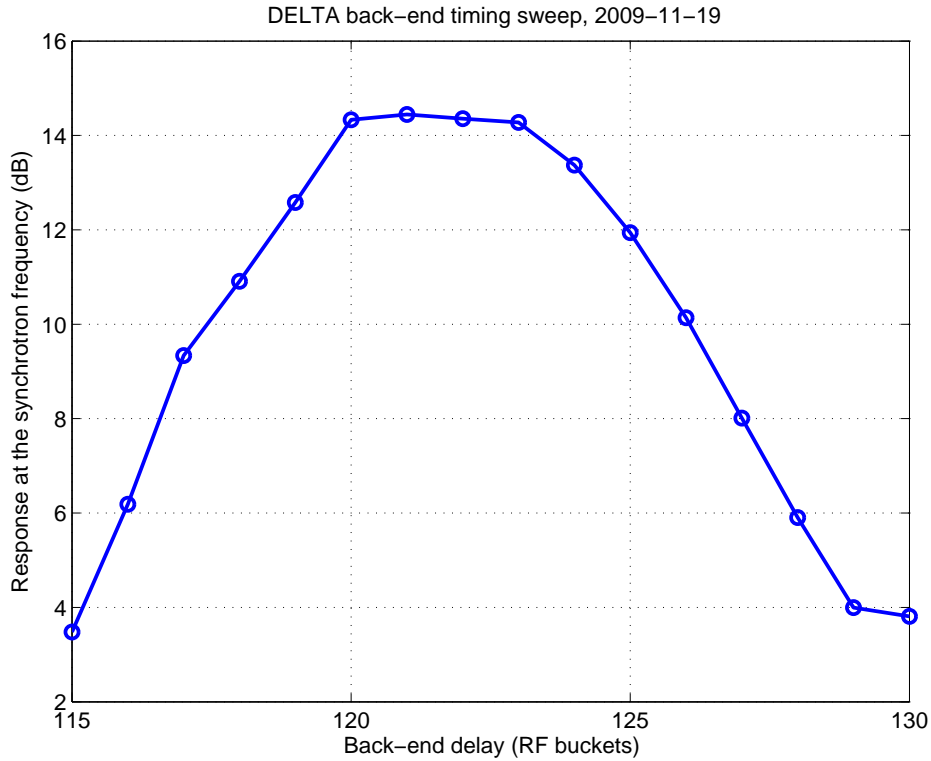


Figure 3: Back-end timing sweep.

and the fine timing adjustment of the DAC to 1000 ps.

2.2 Measurements under the instability threshold

Starting at beam currents of around 5 mA we observed some effect of the feedback on the beam, with the positive feedback exciting the beam motion and the negative feedback damping the synchrotron resonance.

At 31.4 mA we reached a point where positive feedback gain was sufficient to drive the beam to instability, enabling us to perform what is known as drive/damp measurements. The feedback is positive in the first part of the transient and then negative or open-loop in the second part. Resulting data allows us to estimate radiation damping and, roughly, feedback gain. To estimate feedback gain one can use the standard feedback relationship [5]:

2.2 Measurements under the instability threshold

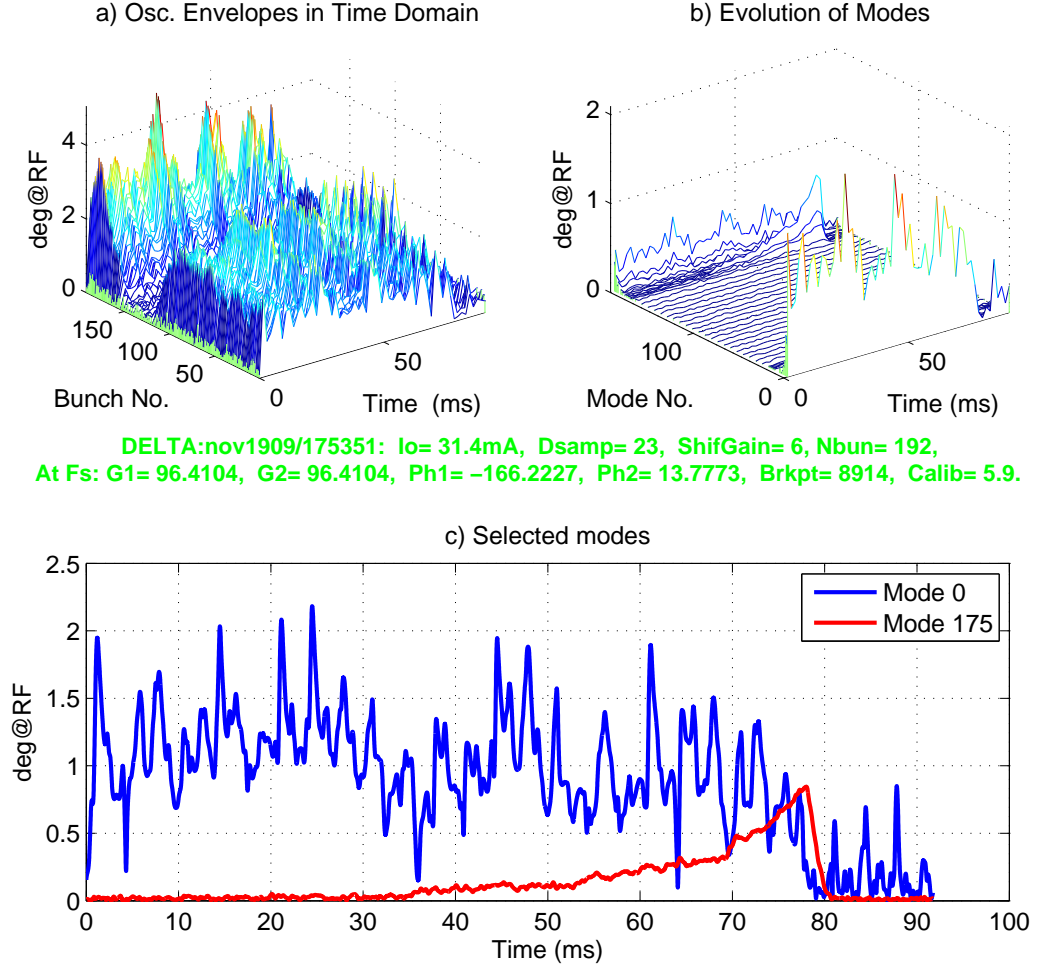


Figure 4: Drive/damp measurement at 31.4 mA.

$$\lambda_{\text{fb}} = \frac{f_{\text{RF}}^2 \alpha e}{2E_0 h f_s} G_{\text{fb}} \quad (1)$$

where λ_{fb} is the magnitude of the eigenvalue shift due to the feedback action.

Figure 4 shows a positive/negative feedback measurement at 31.4 mA. Feedback switches from negative to positive at the beginning of the transient and back to negative at 78 ms. A clear modal peaks are observed around modes 0 and 175. Time-domain evolution of modes 0 and 175 is shown in

plot c). Mode 0 is Robinson-stable, so application of positive and negative feedback amplifies and damps external disturbances. Steady-state motion of mode 0 drops from 1.06 degrees under positive feedback to 0.17 degrees with negative feedback. Mode 175 is clearly driven unstable by positive feedback and exhibits exponential growth. Excited mode corresponds to $f_{\text{RF}} + 175f_{\text{rev}} + f_s = 955.7$ MHz — the peak of the kicker response. Thus, the mode, excited by the positive feedback is consistent with what one would expect based on the feedback loop gain dependence on frequency. Fitting complex exponentials to the growing and damping parts of the transient we extract the eigenvalue of $(58 \pm 0.3) + (96419 \pm 0.3)i \text{ s}^{-1}$ under positive feedback and $(-1330 \pm 10) + (95520 \pm 12)i \text{ s}^{-1}$ under negative feedback. Eigenvalue shift is $1387 + 899i \text{ s}^{-1}$. In this case the effect of the feedback is strongly reactive — typical with positive feedback. Using Eq. 1 we can roughly estimate the feedback gain. The eigenvalue shift of $\sqrt{1387^2 + 899^2} = 1653 \text{ s}^{-1}$ gives us $G_{\text{fb}} = 5.5 \text{ kV/rad}$. Note that the shift magnitude has to be divided by two before substitution into Equation 1, since with positive and negative feedback the eigenvalue shift is doubled.

Two measurements at 42 mA are illustrated in Fig. 5. In one case we excite the beam with positive feedback, then turn the feedback off to observe the natural damping. For the second measurement, negative feedback is applied. Measured eigenvalues for mode 8 are $(-275 \pm 0.5) + (96342 \pm 0.5)i \text{ s}^{-1}$ and $(-1011 \pm 0.5) + (96714 \pm 5)i \text{ s}^{-1}$. Open-loop damping rate measured here corresponds to the damping time of $1/0.275 = 3.64 \text{ ms}$ — reasonably close to the expected radiation damping time of 4.17 ms.

Feedback-induced eigenvalue shift is $736 - 372i \text{ s}^{-1}$ corresponding to a gain of 5.49 kV/rad — in the rough agreement with the drive/damp measurement shown in Fig. 4. Since the earlier measurement was at 34.1 mA vs. 42 mA, we would expect a gain increase of 1.23.

We can use the estimated gain to compute the peak kick voltage. Overall feedback gain is given by

$$G_{\text{fb}} = \frac{V_{\text{max}}}{128} |H_{\text{fir}}(\omega_s)| i_b G_{\text{fe}} \quad (2)$$

where H_{fir} is the FIR filter transfer function, i_b is the bunch current and G_{fe} is the front-end calibration in counts/rad/A. Using these parameters we estimate $V_{\text{max}} = 21 \text{ V}$.

2.3 Measurements above the threshold

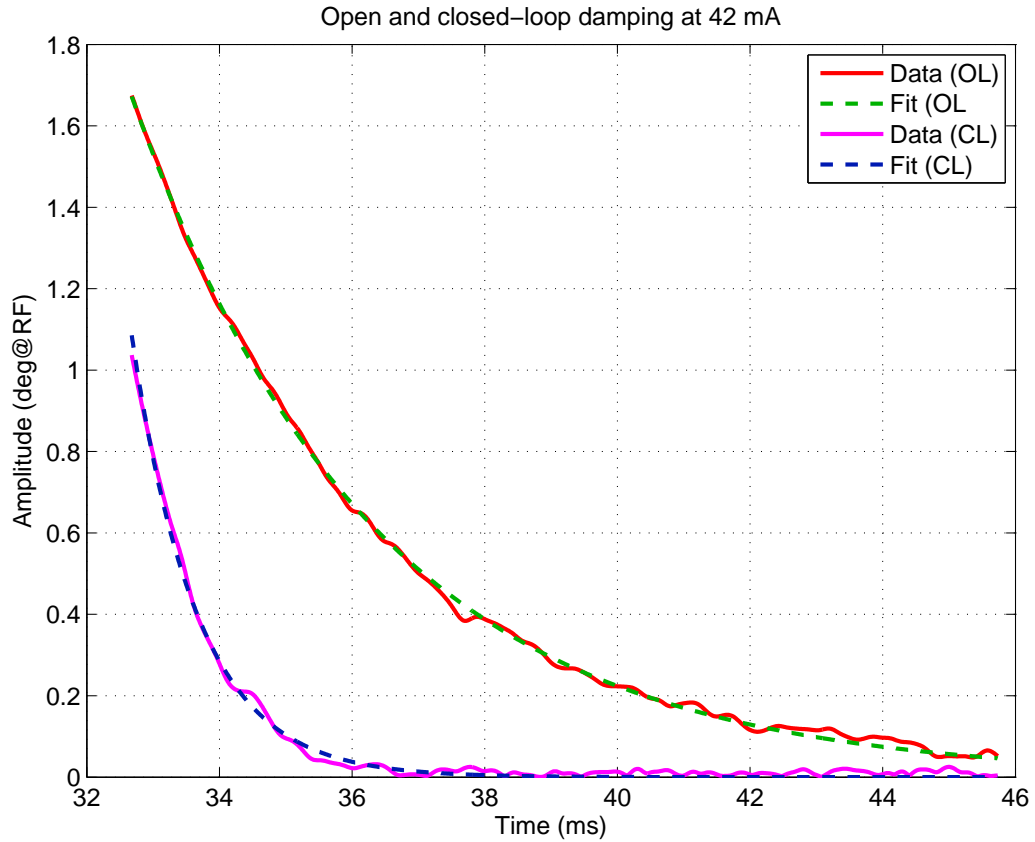


Figure 5: Damping of mode 8 at 42 mA in open-loop and negative feedback conditions. Open-loop damping rate of 0.275 ms^{-1} is shifted by feedback to 1.01 ms^{-1} .

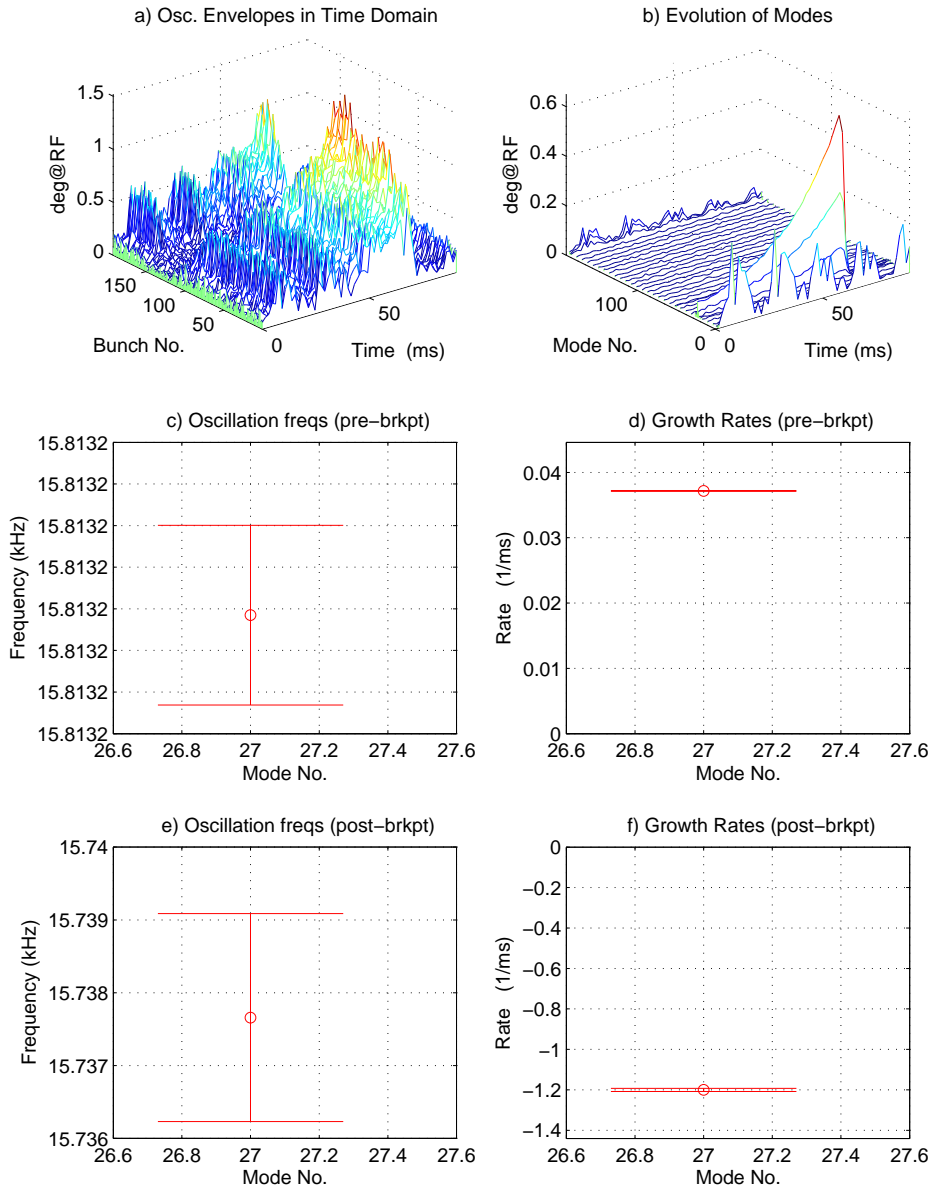
2.3 Measurements above the threshold

At 87.1 mA we have collected the first data set above the instability threshold. Figure 6 shows a grow/damp measurement slightly above the threshold, at 90.1 mA.

A total of 40 grow/damp measurements were collected above the instability threshold. However in the consequent analysis it was determined that the majority of these measurements were performed in the drive/damp configuration (due to an unfortunate operator error).

Using the data sets, acquired before the open-loop configuration was re-

2.3 Measurements above the threshold



DELTA:nov1909/190634: $I_0=90.1\text{mA}$, $D_{\text{samp}}=23$, $\text{ShifGain}=6$, $N_{\text{bun}}=192$,
 At Fs: $G1=107.1332$, $G2=0$, $\text{Ph1}=165.6168$, $\text{Ph2}=0$, $\text{Brkpt}=7930$, $\text{Calib}=5.9$.

Figure 6: Grow/damp measurement at 90 mA.

placed by positive feedback, we generate the plot in Figure 7. Linear fits

to the growth rates and the oscillation frequencies allow us to estimate the zero-current values, which should coincide with the radiation damping and zero-current synchrotron frequency. The fits also provide an estimate of expected growth rates at nominal operating current of 130 mA. Given the low number of current points sampled in these plots, estimates of the radiation damping and the synchrotron frequency agree as well as it could be expected.

There is significant variation in the measured damping rates, most likely due to the back-end saturation of the system. At the gain needed to stabilize the beam the feedback is continuously driven into saturation. Depending on the external excitation during the transient measurement, measured damping rate can vary dramatically. Using one of the measurements at 100 mA with the fast damping rate, we estimate the maximum kick voltage as 13.7 V for mode 54. While this is lower than 21 V estimated in the previous section, one has to remember that kicker shunt impedance has significant frequency dependence. Modes 8 or 175 are near the peak of the kicker impedance, while mode 54, at 859 MHz is almost 100 MHz away from the peak. At this point kicker gain is down by a factor of two. In fact we would expect the voltage to be 10.5 V. Of course, this calculation disregards impedance mismatches, amplifier power variation with frequency and many other possible sources of error.

2.4 Transverse measurements

Even though our front-end input signal is a sum of four BPMs, there is still some residual sensitivity to transverse motion. This sensitivity was used to observe transverse motion and to analyze the modal patterns of unstable motion. Figure 8 shows the modal spectra in the vertical and the horizontal planes, obtained by filtering bunch signals around the respective betatron tunes. In the vertical plane mode 178 is active, while horizontally we observe two modes: 146 and 188. Longitudinal feedback was stabilizing the beam during this measurement.

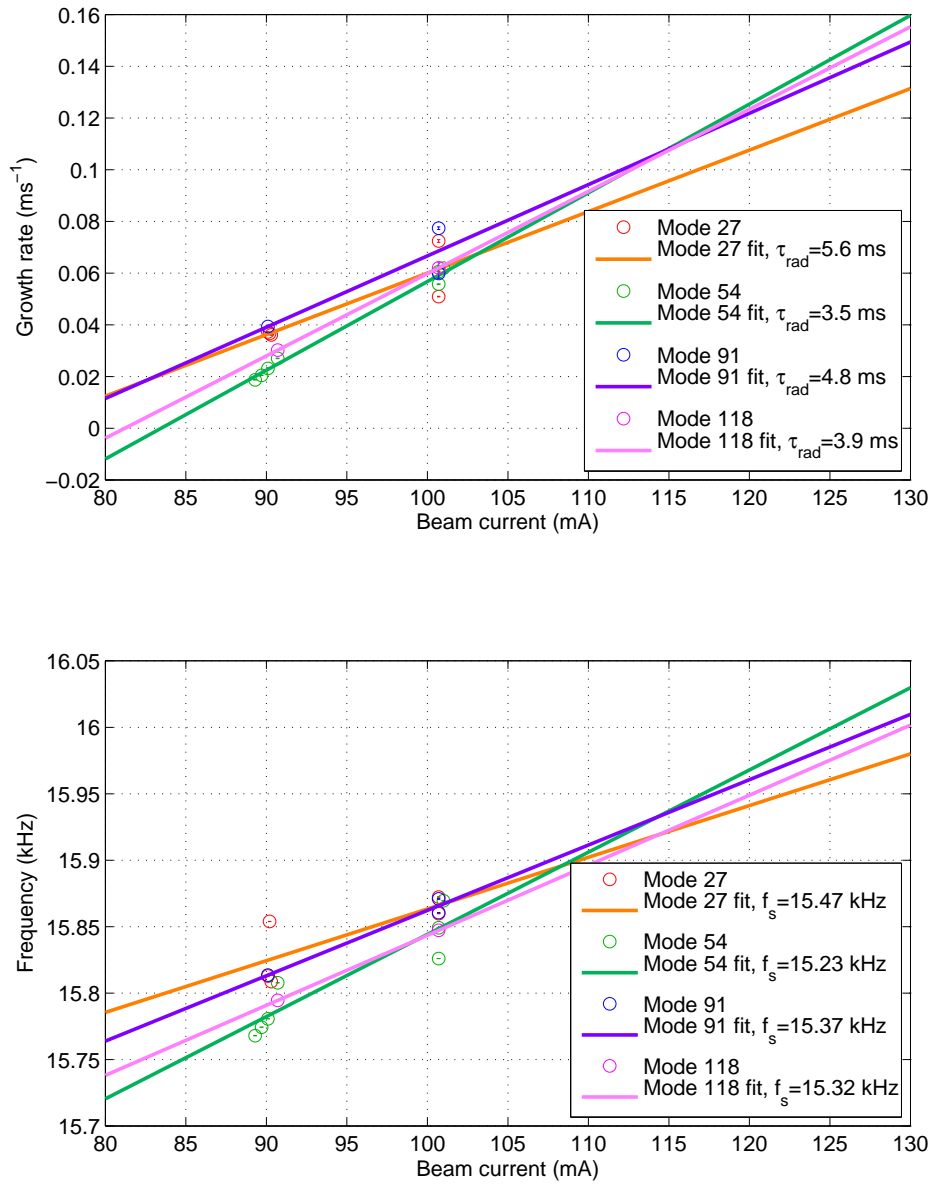


Figure 7: Open-loop growth rates and oscillation frequencies of four unstable modes.

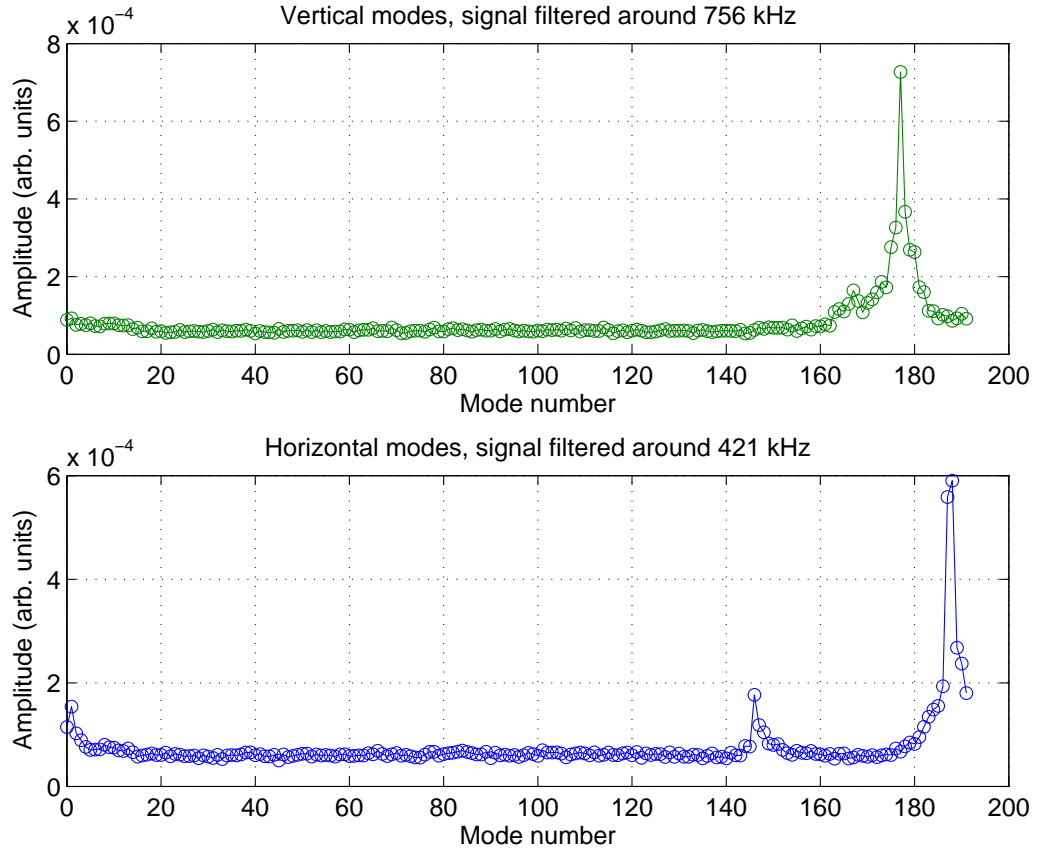


Figure 8: Transverse modal spectra recorded at 131.3 mA.

3 Simulation

3.1 Model

Using grow/damp measurements presented in Section 2 we can calibrate a Simulink model of the unstable beam and the bunch-by-bunch feedback system. Block diagram of the model is shown in Fig. 9. The model is configured with the accelerator parameters from Table 1. Unstable beam mode is set to the growth rate and the oscillation frequency extracted from a particular grow/damp measurement. Feedback system parameters (front-end calibration) are based on the actual beam calibration measurements.

3.2 Simulated grow/damp

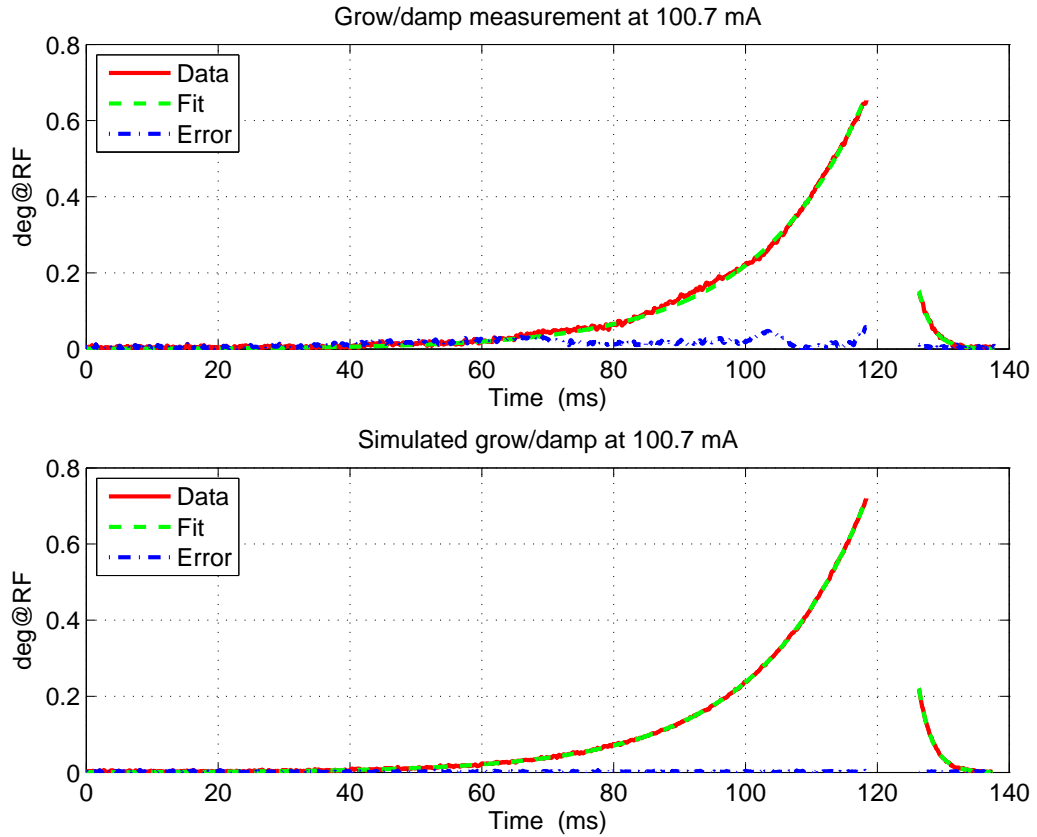


Figure 10: Measured and simulated grow/damp transients at 100.7 mA.

Table 2: Eigenvalues for the measured and simulated grow/damp transients

Parameter description	Measured	Simulated
Open-loop growth rate, ms^{-1}	0.0606	0.0605
Open-loop oscillation frequency, Hz	15848.6	15849.0
Closed-loop damping rate, ms^{-1}	0.475	0.482
Closed-loop oscillation frequency, Hz	15890.2	15887.4

3.3 Steady-state noise

In addition to modeling the open and closed-loop behavior of the instability we also try to match the closed-loop residual motion spectrum. Four noise sources are modeled explicitly. RF wideband noise level is set by the residual beam motion, as measured by the grow/damp transient. Front-end sources model the effects of RF reference noise and detection noise. Front-end noise is a sum of three components: wideband, low-frequency $1/f$ noise, and medium-frequency.

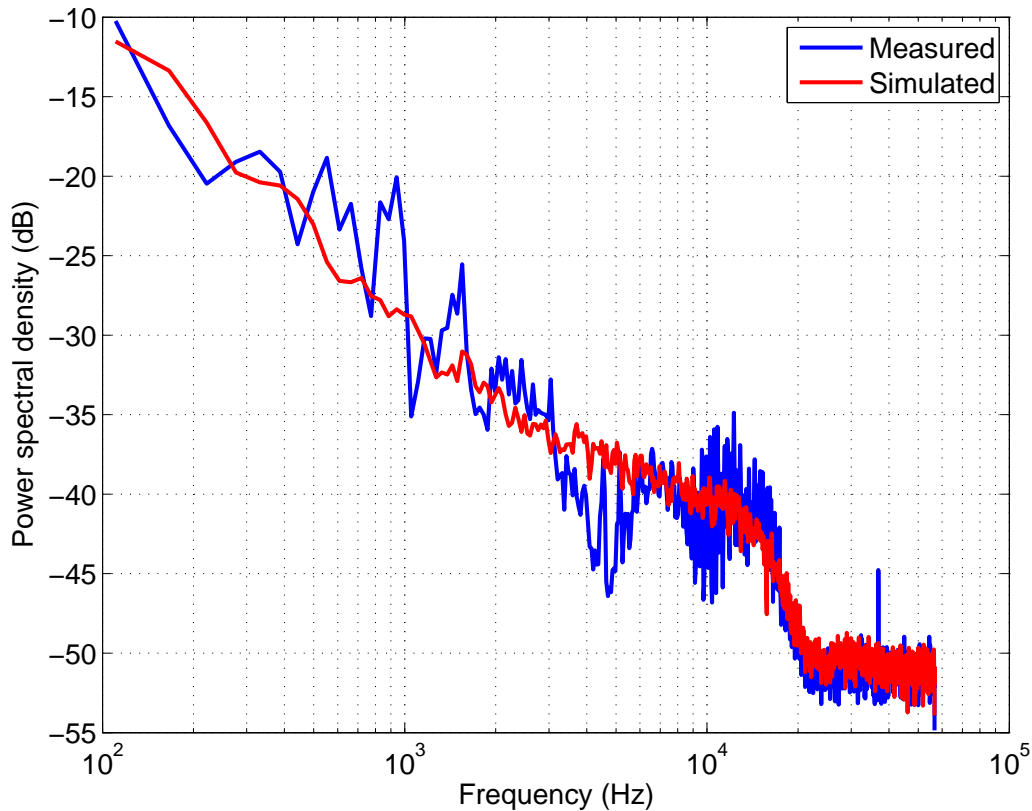


Figure 11: Measured and simulated power spectra.

Figure 11 shows the measured and simulated power spectra. Measured spectrum is computed from a single bunch time-domain record of 380 ms at the beam current of 86 mA. The same time span is then simulated under the

3.3 Steady-state noise

closed-loop conditions.

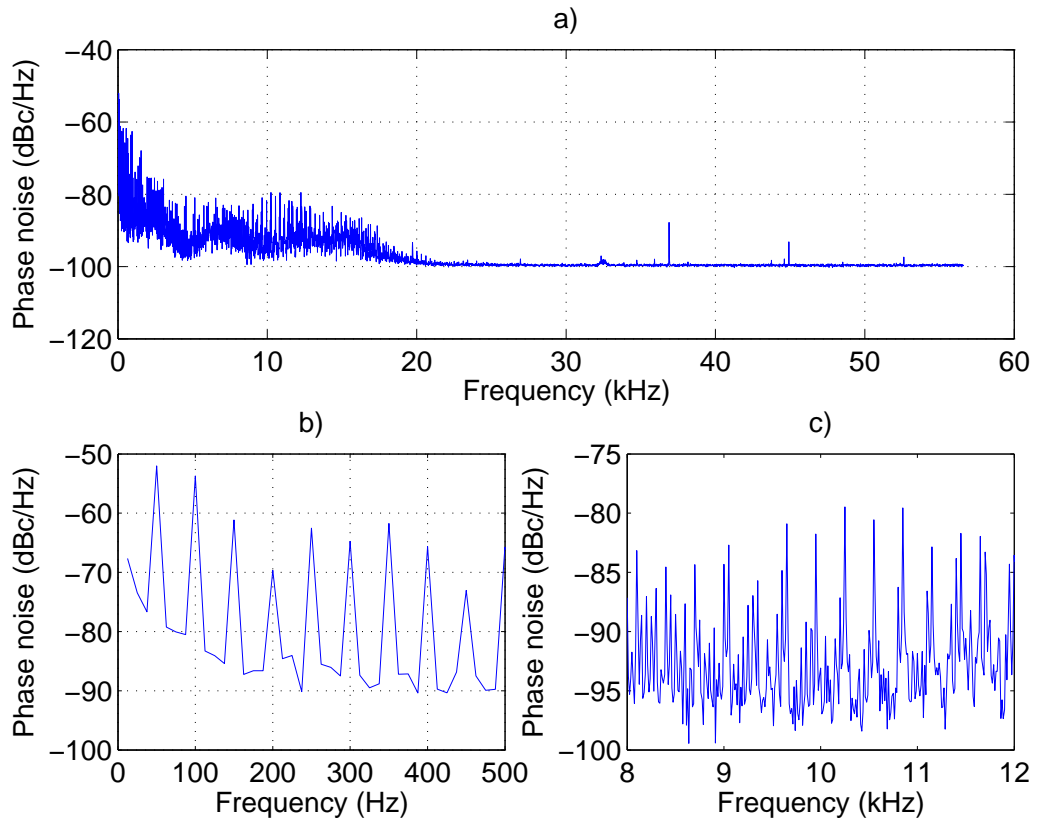


Figure 12: a) Power spectrum density averaged over all filled bunches; b) low-frequency portion of the spectrum showing 50 Hz harmonics; c) medium-frequency range is dominated by 250 Hz harmonics.

It is important to note that Fig. 11 shows excessive phase noise at low frequencies, with a relatively flat spectrum extending to 17 kHz. That noise spectrum is best seen against a linear frequency axis, as shown in Figure 12. Part of this spectrum is due to the noise on the RF reference signal supplied to the feedback system. The rest part is most likely driven on the beam by the RF system. For example, 50 Hz harmonics at low frequencies are most likely due to the reference, while 250 Hz lines might be generated by the high-voltage power supply (HVPS) ripple.

3.4 Extrapolation

Typically the kick voltage estimated from grow/damp measurements and the model is used to calculate the kicker shunt impedance using Eq. 3.

$$R_s = \frac{V_{\max}^2}{2P} \quad (3)$$

However in the case of the DELTA improvised kicker such calculation is extremely difficult. Input power P in this case depends on the unknown characteristic impedance of the stripline.

Therefore we omit this calculation and use the calibrated model to predict the performance of the longitudinal feedback system with a wideband kicker. Kicker shunt impedance is assumed to be 680Ω — BESSY-II kicker shunt impedance reduced by 3 dB [6]. Two power amplifiers — with P_{1dB} of 5 W and 25 W — have been tested in the simulation.

Figure 13 shows simulated grow/damp transients at 150 mA. From the measurements shown in Fig. 7 we estimate the highest growth rate at that current as 0.23 ms^{-1} for mode 54. Both amplifiers provide excellent damping margins. Feedback controller gain has been lowered relative to the demonstration setup to keep the system well out of saturation in the steady state.

In Fig. 14 simulated transients at 200 mA are shown. Again, both amplifiers provide sufficient damping. Note that no effort has been made to optimize the feedback controller phase for resistive damping. Optimized feedback controller should improve the overall damping by roughly 25%.

During the demonstration we observed that the beam could be successfully stabilized up to the maximum operating current of 130 mA. This observation reinforces the conclusion that very low amplifier power is needed with a dedicated kicker. Shunt impedance is at least 20 to 100 times larger with the real kicker, allowing a similar reduction in the amplifier power.

At the power levels of 5–25 W relatively inexpensive amplifiers are available. Mini-Circuits ZHL-5W-2G-S+ produces 5 W from 800 to 2000 MHz and is priced at \$995 — just add a power supply and an enclosure. At \$2995 ZHL-30W-252-S+ provides 25 W from 700 to 2500 MHz.

4 Summary

Operation of the iGp-192F bunch-by-bunch feedback processor and the FBE-500L front/back-end has been successfully demonstrated at DELTA. Longi-

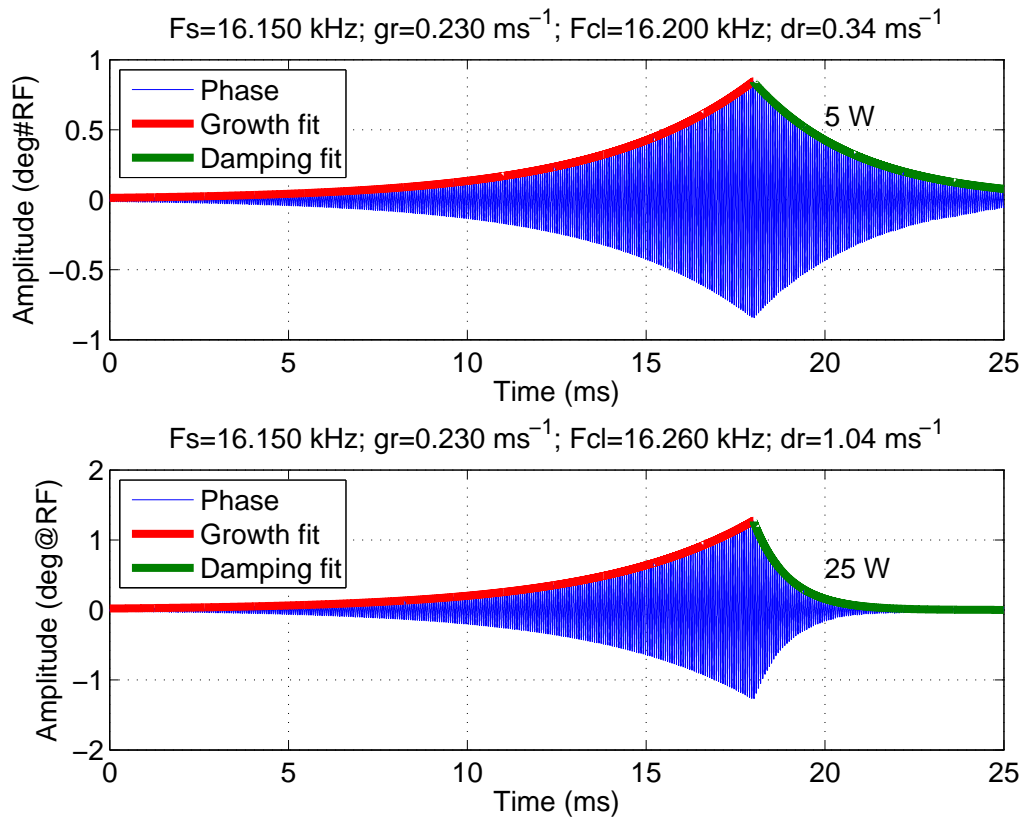


Figure 13: Simulated grow/damp transients at 150 mA beam current.

tudinal coupled-bunch instabilities have been characterized both below and above the instability threshold. Bunch-by-bunch diagnostic data has also been used to analyze the transverse modal patterns above the respective instability thresholds.

Measured instability growth rates and closed-loop steady-state spectra have been used to configure an off-line model of the beam and the feedback system. The model has then been used to estimate power amplifier and kicker requirements for production running of the accelerator under feedback control.

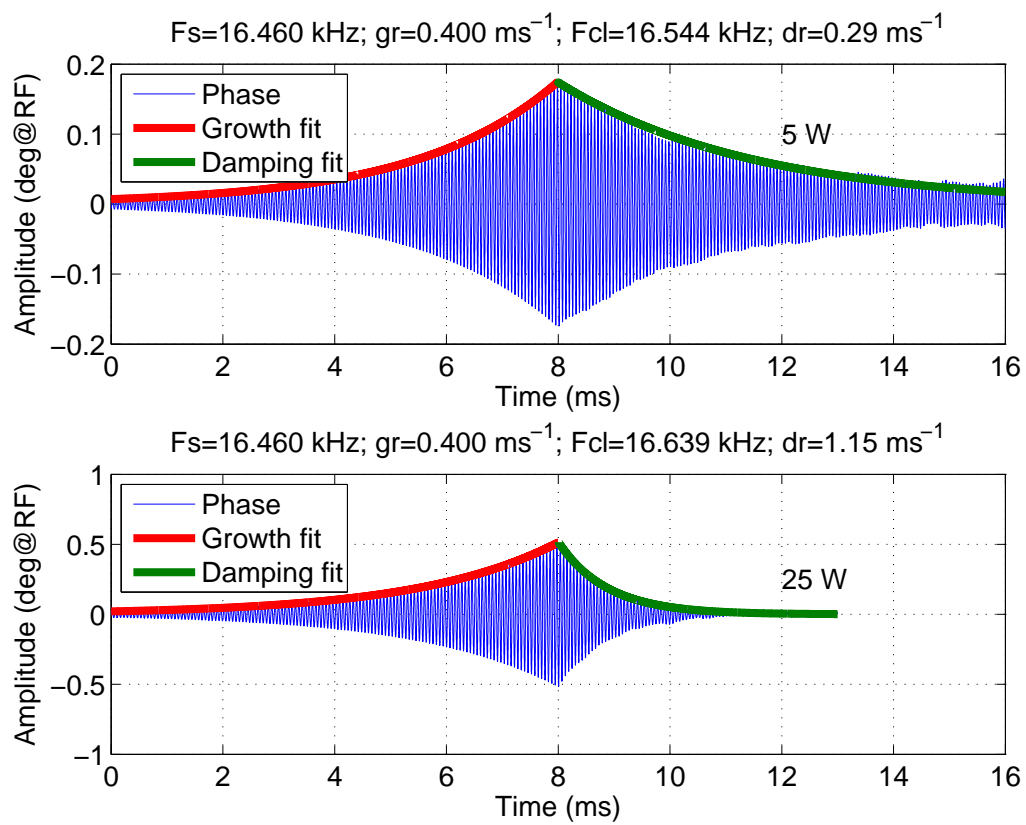


Figure 14: Simulated grow/damp transients at 200 mA beam current.

5 Glossary

Glossary

high-voltage power supply (HVPS)

A power supply for the high-power amplifier (klystron or inductive output tube (IOT)), typically operating in multi-kilovolt high-current range 16

inductive output tube (IOT)

A high-efficiency vacuum tube used for high-power RF amplification 20

References

- [1] <http://www.dimtel.com/products/igp>.
- [2] P. Hartmann, J. Fürsch, R. Wagner, T. Weis, and K. Wille, “Kicker based tune measurement for DELTA,” in *DIPAC 2007: Proceedings*, (Trieste, Italy), pp. 277–279, ELETTRA, 2007.
- [3] G. Blokesch, M. Negrazus, and K. Wille, “A Slotted pipe kicker for high current storage rings,” *Nucl. Instrum. Meth.*, vol. A338, pp. 151–155, 1994.
- [4] http://www.dimtel.com/products/longitudinal_fbe.
- [5] S. Prabhakar *et al.*, “Observation and modal analysis of coupled-bunch longitudinal instabilities via a digital feedback control system,” *Part. Accel.*, vol. 57, p. 175, 1997.
- [6] S. Khan *et al.*, “Longitudinal and transverse feedback kickers for the BESSY II storage ring,” in *Proceedings of the 1999 Particle Accelerator Conference*, (Piscataway, NJ, USA), pp. 1147–1149, IEEE, 1999.